JATIS Journal of Astronomical Telescopes, Instruments, and Systems

RESEARCH PAPER

Arcus ultraviolet spectrograph: enabling far-ultraviolet spectroscopy with the Arcus X-ray probe

Kevin France[a,*] **Brian Fleming**[a] **Laura Brenneman**[b] **Randall Smith**[b] **Joel Bregman**[c] **Nancy Brickhouse**[b] **Hans Moritz Günther**[d] **Todd M. Tripp**[e] **Dolon Bhattacharyya**[a] **Timothy Hellickson**[a] **Nicholas Nell**[a] **Tom Patton**[a] **Katja Poppenhaeger**[f] **and Pasquale Temi**[g]

[a]University of Colorado, Laboratory for Atmospheric and Space Physics, Boulder, Colorado, United States
[b]Smithsonian Astrophysical Observatory, Cambridge, Massachusetts, United States
[c]University of Michigan, Department of Astronomy, Ann Arbor, Michigan, United States
[d]MIT Kavli Institute for Astrophysics and Space Research, Cambridge, Massachusetts, United States
[e]University of Massachusetts, Department of Astronomy, Amherst, Massachusetts, United States
[f]Leibniz Institute for Astrophysics Potsdam, Potsdam, Germany
[g]NASA Ames - Astrophysics Branch, Moffett Field, California, United States

ABSTRACT. Arcus is a high-resolution soft X-ray and far-ultraviolet spectroscopy mission submitted to the National Aeronautics and Space Administration's inaugural Astrophysics Probe solicitation. Arcus makes simultaneous observations in these two critical wavelength regimes to address a broad range of science questions highlighted by the 2020 Astronomy and Astrophysics Decadal Survey, from the temperature and composition of the missing baryons in the intergalactic medium to the evolution of stars and their influence on orbiting planets. We present the science motivation for and performance of the Arcus ultraviolet spectrograph (UVS). UVS comprises a 60-cm, off-axis Cassegrain telescope feeding an imaging spectrograph operating over the 970- to 1580-Å bandpass. The instrument employs two interchangeable diffraction gratings to provide medium-resolution spectroscopy ($R > 20{,}000$ in two grating modes centered at ~1110 and 1390 Å). The spectra are recorded on an open-face, photon-counting microchannel plate detector. The instrument design achieves an end-to-end sensitivity >10 times that of the Far-Ultraviolet Spectroscopic Explorer over the key 1020- to 1150-Å range and offers arcsecond-level angular resolution spectral imaging over a 6-arcminute-long slit for observations of extended sources. We describe the example science investigations for far-ultraviolet spectroscopy on Arcus, the resultant instrument design and predicted performance, and simulated data from potential General Observer programs with Arcus.

 [DOI: 10.1117/1.JATIS.11.1.011002]

Keywords: astrophysics probes; X-ray and far-ultraviolet; spectroscopy; black holes; circumgalactic medium; exoplanet host stars

Paper 24063SS received May 10, 2024; revised Jul. 26, 2024; accepted Aug. 5, 2024; published Sep. 26, 2024.

1 Introduction

The 2020 decadal survey[1] highlighted three key science themes for astronomy and astrophysics in the 2020s and 2030s: cosmic ecosystems, worlds and suns in context, and new messengers and

*Address all correspondence to Kevin France, kevin.france@colorado.edu

new physics. The decadal survey illustrated that all three themes drive the need for high-sensitivity and high-resolution spectroscopy at X-ray and far-ultraviolet wavelengths to achieve the most pressing astronomical challenges of the next 20 years. Arcus is a joint X-ray and far-ultraviolet mission concept designed to respond directly to these themes. The 5-year baseline science and general observer mission was proposed to the National Aeronautics and Space Administration (NASA) as part of the first Astrophysics Probe opportunity in late 2023.

Within the cosmic ecosystems theme, investigating the cycling of materials into and out of galaxies ("feedback") and how this process is connected to galaxy evolution and the properties of central supermassive black holes is listed as the priority area. Arcus aims to unveil the drivers of galaxy growth and evolution by (1) studying how winds from supermassive black holes in active galactic nuclei (AGNs) are launched and impact their galactic environments and (2) understanding how cool, warm, and hot gases are driven into the halos of galaxies, how those halos interact with the larger intergalactic medium, and ultimately how those gases are recycled into future generations of stars. In the area of worlds and suns in context, Arcus will reveal the physics of stellar mass accretion, how stellar atmospheres are heated and the impact on orbiting exoplanets, and how the winds of massive stars interact with their galactic environments and ultimately contribute to the evolution of the cosmic ecosystem.

These high-priority science investigations require simultaneous spectral data at soft X-ray (10 to 60 Å) and far-ultraviolet (FUV; 970 to 1580 Å) wavelengths. However, owing to the material properties of optics and detectors, no single instrument can accommodate both bandpasses. Arcus achieves the required, simultaneous wavelength coverage with two co-aligned telescopes. These instruments are designed with optimized collecting mirrors, gratings, and detectors, supported by ground reconstruction of the photon-counting detector data, to achieve the required spectral resolution, effective area, and background levels to carry out these investigations. Arcus' X-ray spectrometer (XRS) instrument is described in a companion paper (see Smith et al., this volume). Arcus' ultraviolet spectrograph (UVS) instrument employs an off-axis Cassegrain telescope using coatings specifically designed for high reflectivity in the FUV. UVS uses standard diffraction gratings with holographically etched grooves. Both instruments employ high-sensitivity photon-counting detectors. The XRS and UVS data are calibrated and delivered to the astronomical community through High Energy Astrophysics Science Archive Research Center and Mikulski Archive for Space Telescopes.

This paper describes example science investigations to be carried out by Arcus, which are enabled by simultaneous observations at X-ray and FUV wavelengths (Sec. 2), with an emphasis on the science drivers for the FUV capabilities of the mission with the UVS. These example science investigations are followed by a description of the UVS instrument package in Sec. 3 (see also Fleming et al.—this issue—for technical details of the UVS design). We conclude in Sec. 4 by providing simulated data and science performance metrics for the UVS instrument, for example, science investigations that could be submitted to Arcus' general observer call for proposals.

2 Example Science Investigations with High-Resolution X-ray and FUV Spectroscopy

The Arcus Probe science mission provides transformative discoveries across a wide range of astrophysical phenomena, from the physics of black hole outflows to the distribution of gas in the halos of galaxies and the cycle of cosmic star formation and to the physics of how young stars grow and ultimately affect orbiting planetary systems (Secs. 2.1–2.3). These science goals require simultaneous spectroscopic observations at X-ray and ultraviolet (UV) wavelengths to access the most important physical tracers of these objects and with sufficient sensitivity to measure how these objects evolve on their characteristic timescales (minutes to days). High spectral resolution is necessary to separate closely spaced emission and absorption lines and distinguish these from adjacent continuum regions. We provide three representative, but by no means complete, examples of science investigations enabled by the combined X-ray and FUV capabilities of the Arcus XRS and UVS instruments.

2.1 Supermassive Black Hole Feedback

The tight correlation between supermassive black hole (SMBH) mass and stellar velocity dispersion of host galaxy bulges[2–4] reveals that black holes and galaxies have co-evolved. Foundational numerical simulations[2] show that accretion-powered wind feedback, equivalent to just 1 to 5% of the radiative luminosity, can reshape host galaxies and drive co-evolution, sweeping the bulge of cold gas and preventing future star formation. For accretion-driven winds to govern the coevolution of SMBHs and host galaxies, they must be relatively common and act over many orders of magnitude in physical scale, connecting regions close to the black hole to kpc scales (Fig. 1). In connecting those scales, winds must eventually entrain additional gas and dust, losing speed as they conserve momentum, and they must eventually act over a broad range in solid angle. The total mass outflow rate and kinetic power are set in the "upstream" flow, connected to the accreting SMBH. Emission from the central corona peaks at X-ray wavelengths whereas the innermost disk is brightest at FUV wavelengths; therefore, the innermost accretion flow and the winds it generates are best revealed by sensitive atomic spectra in the X-ray and FUV.

The X-ray grating spectrometers aboard Chandra and XMM-Newton and the UV Cosmic Origins Spectrograph aboard Hubble Space Telescope (HST) have provided a few key glimpses into wind-driven feedback in a handful of sources where sensitive spectra can be obtained. In those sources (e.g., the Seyfert 1 galaxy NGC 5548), there is evidence of similar velocity structure in UV and X-ray absorption lines, indicating a complex, multi-phase outflow that requires study in both wavelength regions.[5–7] X-ray and UV winds can be broken into two distinct velocity regimes: fast ($v_{\rm out} > 10{,}000$ km s^{-1}) and slow ($v_{\rm out} < 10{,}000$ km s^{-1}). Slower winds include "warm absorber" winds, obscurers, and "broad line region" (BLR) winds.[8] Faster winds include ultra-fast outflows (UFOs), which are typically detected in X-rays and UV (e.g., Refs. 9 and 10), and broad absorption lines (BALs), which are only seen in the UV.[11] Possible origins of these fast and slow outflows are schematically depicted in Fig. 1. However, the

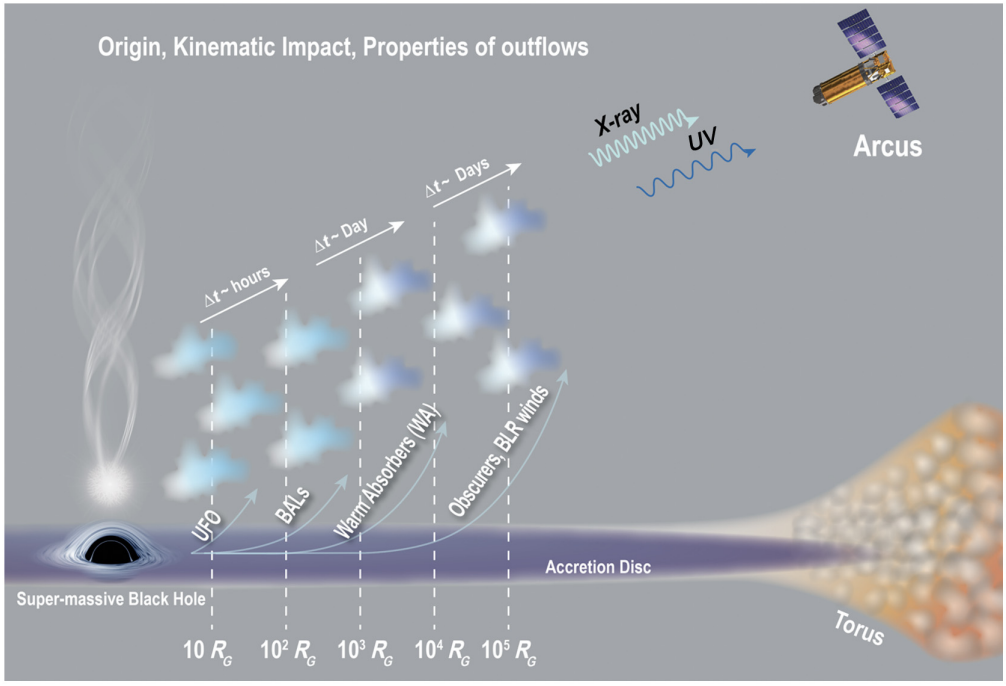

Fig. 1 Schematic diagram of an AGN central engine, including the supermassive black hole (black), the accretion disk (purple), the torus (orange), and the winds (white and blue). Arcus will reveal how winds are launched and how they are layered; this diagram assumes that the fastest winds are launched from the smallest radii. From left to right, the diagram shows the UFOs, BALs, warm absorbers, and narrow absorption lines. The diagram also depicts the different time scales (hours, day, days) at which Arcus will be able to capture the evolution of such clouds in conjunction with the variations in the AGN continuum. The ability to study the ionizing continuum and wind spectra simultaneously in X-rays and FUV is essential to all aspects of revealing wind feedback from AGN.

available energy resolution and sensitivity of current X-ray spectrometers, coupled with their lack of simultaneous UV spectral coverage, make it impossible to obtain reliable measurements of the two quantities that determine the feedback delivered by time–variable accretion-driven winds: the total mass outflow rate and kinetic power at $E < 3.0$ keV ($\lambda > 4$ Å). Arcus is designed to provide these key missing data.

Arcus will conduct two primary supermassive black hole surveys to answer key questions about the launching and structure of their winds. The AGN broad sample (ABS) obtains the first meaningful census of accretion-driven winds in local SMBHs, and the AGN deep sample (ADS) will obtain the first direct constraints on wind launching radii, gas densities, and thereby true mass outflow rates and kinetic powers. These samples are selected to span key ranges in black hole mass, Eddington fraction, and viewing angle and to pair optimally with observations in optical, infrared, and sub-millimeter bands that can trace wind feedback on kpc scales.

The ABS will observe 160 AGN simultaneously with XRS and UVS to begin answering these questions and to establish a reference for General Observer investigations. It will deliver the first unbiased census of X-ray and FUV wind velocities, ionizations, and column densities in local AGN. The sample is centered on an Eddington fraction of $\lambda_{\rm Edd} = 0.3$ but spans an order of magnitude in each direction, covering the full range where AGN feedback is expected to have the largest impact on host galaxies.[2,12] Similarly, the sample is centered on a redshift of $z = 0.05$ but extends up to $z = 0.3$. The UV fluxes at 1050 Å of the ABS sample are in the range $(0.1 \text{ to } 4.5) \times 10^{-14}$ erg cm^{-2} s^{-1} Å^{-1}, with a typical value of about 1×10^{-14} erg cm^{-2} s^{-1} Å^{-1}.

The synergy between XRS and UVS will offer a unique view of virtually all ionization states of the most abundant elements and major products of stellar evolution: carbon, nitrogen, and oxygen with both the XRS and UVS, and iron with the XRS. At the same time, hydrogen, a major tracer of any type of wind, will be covered by UVS (via Lyα and Lyβ). Exposure times on these sources are driven by the X-ray observing duration, with ABS exposure times in the range of 10 to 90 ks, enabling both UVS gratings to be used to cover the full suite of UV ions (depending on the target redshift, Sec. 3).

The ADS utilizes the same observing strategy yet acquires spectra several times deeper (with a sample size of ~30 AGNs) to track time variability in wind absorption lines and the corresponding changes in wind density. The ADS will study 30 bright, unobscured AGNs, selected on their X-ray characteristics using the following criteria: (1) strong variability on 10-ks timescales (producing multiple expected significant flux changes in a long observation) and (2) detection of 10% variations in O VII and O VIII absorption lines with $t_{\rm exp} < 300$ ks. This preliminary list of targets was then refined to ensure that it samples the same range in black hole mass and Eddington luminosity as the ABS; however, the average AGN in the ADS will be observed for ~300 ks, ~10× deeper than sources in the ABS. Each survey has a projected total observing time duration of 8 to 9 Ms.

2.2 Warm Gas and Metals Cycling into and Out of Galaxies

Most galactic baryons are in hot or "warm–hot" phases (10^5 to 5×10^6 K) and reside in a circumgalactic medium (CGM) that extends to at least the virial radius (250 kpc for a Milky Way–type galaxy). The column densities are significant, but the mean density is low; detection of these "missing baryons" through absorption in the X-ray and FUV spectral regions with access to these temperatures is the most powerful technique for inferring the abundance, temperature, and kinematics of this gas in galaxy halos and at the interface with the intergalactic medium. UV absorption studies have enabled significant progress (e.g., Refs. 13 and 14), providing evidence that halos of galaxies, groups, and clusters are filled with multi-phase and metal-enriched gas clouds. However, UV observations alone cannot constrain the hottest phases of the CGM where most of the metals and baryons are expected to be found. Arcus will fill this important gap, providing sensitive X-ray and FUV spectroscopy with the gas temperature coverage and spectral resolution required to study the physics of gas outflows and inflows as well as the volume-filling hot gas of galaxy halos and beyond.

Models predict that such halos are present over a wide range of galaxy masses. In general, the gas mass increases with the total gravitating halo mass, but there are significant disagreements between models.[15] For sub-L* galaxies (where L* is the characteristic luminosity of a Milky Way–like galaxy), the CGM baryon mass fraction varies by ~3× between recent

EAGLE and IllustrisTNG cosmological hydrodynamic simulations; for galaxies above L*, differences of ∼2× persist. Comparable discrepancies exist between observations and semi-analytic models.[16–19]

Arcus will provide the first comprehensive dataset for distinguishing among models of the CGM, which have very different ion signatures across the array of species probing hot gas between $T = 10^5 - 10^7$ K (Fig. 2). Observations through the Milky Way's hot halo indicate that about half of the baryons are bound to the galaxy, but there is significant uncertainty, and other L* galaxies may be different.[22] The joint X-ray and FUV spectra from Arcus will provide the first comprehensive census of these different temperature phases across a statistical sample of galaxies in the low-redshift universe. We refer the reader to the mission overview paper by Smith et al. (this volume) for additional survey descriptions.

Arcus will uniquely measure the observational signatures of feedback in the halo gas: its temperature, the shape of its density distribution, and its metallicity. The ejection of ∼80% the metals produced by stars[23] should ensure that metal-enriched gas is extensive, a result observationally supported by a flattened distribution of lower-temperature, O VI-bearing gas, out to ≳160 kpc.[24] UVS will directly measure the H I and metal lines in the FUV, which will tightly constrain the metallicity of the cooler and warm–hot gas.

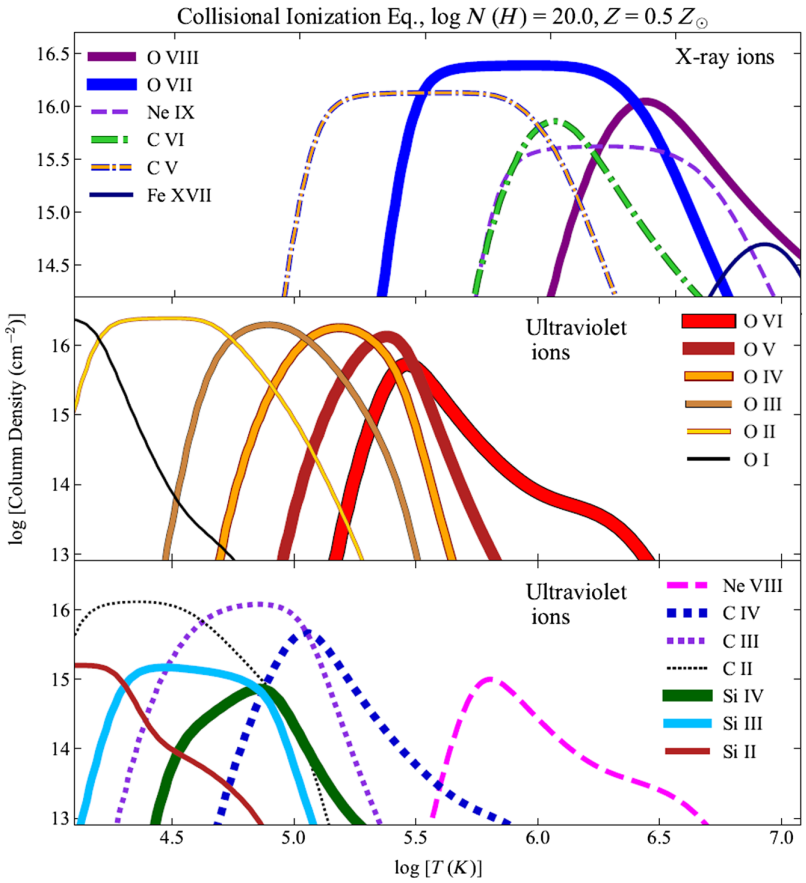

Fig. 2 Arcus will determine the amount and temperature of hot gas in galaxy halos, groups, periphery of clusters, and cosmic web filaments over a range of redshifts. The X-ray lines sample the volume filling gas (near the virial temperature) whereas the FUV lines primarily sample transition gas, arising from radiative cooling and feedback (all species noted here are covered by Arcus at low-to-intermediate redshift). The simultaneous X-ray and UV data and the spectral coverage of UVS enable observations of lines with a range of strengths (constraining line saturation using the weaker lines) while simultaneously providing the ability to detect low-metallicity/low-density gas (using the stronger lines). Column densities of selected ions observable with Arcus assume the typical total hydrogen column density and metallicity observed in the COS-Halos survey[20] and the collisional ionization equilibrium ionization models from Oppenheimer and Schaye.[21] Arcus is sensitive to all of these ions at the column densities shown.

The range of expected thermal line widths (e.g., O VI, H I Lyman-series lines, O VII, O VIII, and C VI), potentially narrow lines arising in cool gas, and complex multi-phase component structure require velocity resolution <18 km s^{-1} ($R > 17{,}000$ at 1050 Å sufficient to measure the width of thermally populated O VI absorbers) and spectral coverage from 1020 to 1340 Å to access low-redshift absorption systems of O VI and Lyβ. Absolute wavelength calibration requirement of 15 km s^{-1} (51 mÅ at O VI) enables robust measurements of the kinematic flows within the CGM. UVS will acquire S/N > 10 per resolution element (at 1050 Å, with $R > 20{,}000$) in a characteristic 100-ks observation in the G110M grating (covering O VI and Lyβ for the majority of absorption systems sampled by Arcus), for sources with GALEX FUV magnitudes <18.8, assuming a flat FUV spectrum. By comparison, HST-cosmic origins spectrograph (HST-COS) achieves a similar S/N at 1150 Å with $R \sim 15{,}000$ in ≈20 ks, but without coverage of low-redshift O VI or Lyβ.

Type II GRB UV afterglows,[25] which will supplement the known list of AGN background sources, are estimated to be at a flux level of 5×10^{-15} erg cm^{-2} s^{-1} Å^{-1} at 10 ks post-explosion, which will permit high S/N (∼20 per resolution element) absorption line profiles for the whole range of background sources targeted by Arcus. Arcus will acquire spectroscopic GRB afterglows less than 24 h post-trigger.

2.3 High-Energy Activity of Planet-Hosting Stars

X-ray and FUV spectra with high resolution and sensitivity can characterize the physical conditions of stellar coronae as well as the dynamical processes driving other magnetic phenomena such as flares, winds, and coronal mass ejections. Magnetic activity is the primary stellar driver for atmospheric chemistry and physics on exoplanets. In some cases, stellar X-ray and stellar extreme-UV (EUV) radiation can remove gas faster than it can be replenished,[26,27] a process that likely drives the distribution of short-period planets[28] and may determine the ultimate habitability of temperate, terrestrial planets.[29] At the same time, FUV radiation drives photochemistry and the formation of atmospheric hazes and biosignature gases.[30–32]

The 2020 Astrophysics Decadal Survey's priority area for the "worlds and suns in context" science theme, pathways to habitable worlds, includes the recommendation for the Habitable Worlds Observatory (HWO). In describing this key science theme, the decadal survey emphasized "The pathway to searching for biosignatures on habitable worlds depends strongly on the properties of their parent stars." Characterization of HWO target stars fulfills a key NASA precursor science goal for HWO (#2 precursor observations of infrared/optical/ultraviolet (IROUV) Exoplanet Imaging Targets: "sensitive X-ray and far-UV characterization of stellar radiation environments in the target systems" (NASA Precursor to Pathways Science Gap Summary 2022), and will have a profound influence on the interpretation of exoplanet spectra observed with current [James Webb Space Telescope (JWST)] and future (HWO) great observatories.

The Arcus coronal star sample (CSS) facilitates studies of coronal structure and heating for a rich distribution of ≈50 stars of different ages and types. The sample will include many of the highest priority targets for the HWO, explicitly facilitating atmospheric studies for known planets while also expanding coronal spectral studies conducted by Chandra, XMM-Newton, HST-COS, far-ultraviolet spectroscopic explorer (FUSE), and other observatories.[33–35]

The broad coverage of elements and ionization states provided by joint X-ray and FUV spectroscopy will allow us to determine the emission measure distributions (EMDs; the amount of emitting plasma at a given temperature in a collisional, coronal environment) with unprecedented simultaneous temperature sampling and for stars with low-to-intermediate activity levels. Owing to biases in primary exoplanet detection techniques, low-activity stars host many of the best-studied exoplanetary systems.[35–37] The Arcus dataset enables the calculation of the EUV environments which are the dominant drivers of atmospheric mass loss on all types of planets[38] (Fig. 3). Arcus therefore measures two high-priority bands needed for exoplanet atmosphere modeling and provides the best constraints on the critical EUV band, where no current observational capability currently exists.

Arcus will answer key questions in stellar physics about coronal heating mechanisms by measuring multiple weak dielectric recombination lines in the X-ray. These data provide coronal temperatures accurate to 10% and can be used to derive the degree of ionization equilibrium when paired with EMD analyses over the 10^4 to 10^7 K covered by XRS and UVS.[41]

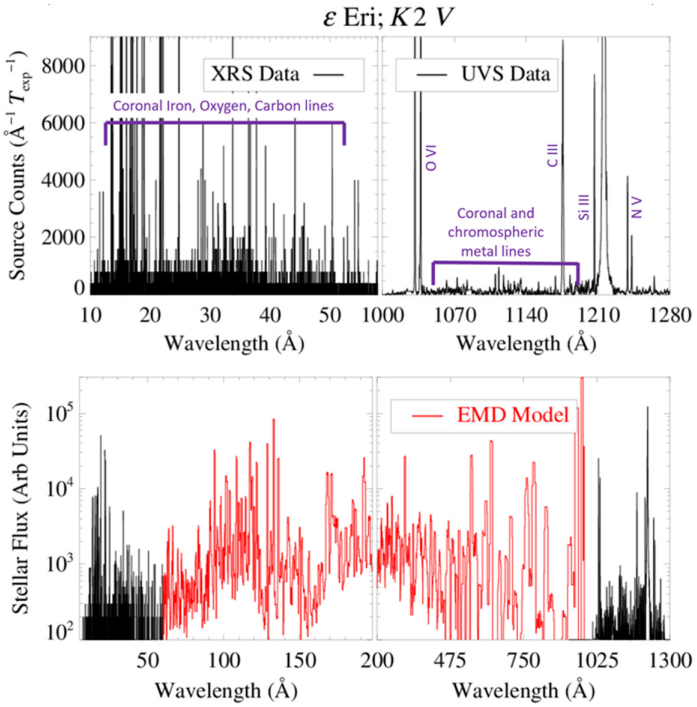

Fig. 3 Simulated Arcus data for the representative K-type star ϵ Eridanus for an exposure time of 5000 s (we note that most stars are X-ray/UV fainter than ϵ Eridanus, and exposure times 10 to 20 times longer are budgeted for most stellar sources). Top panels: Arcus XRS and UVS (G110M) spectra are shown at left and right, respectively, in units of total counts per angstrom in the 5000-s exposure. Simultaneous, high signal-to-noise soft X-ray and FUV inputs enable high-fidelity emission measure distribution analyses[39,40] and spectral synthesis of the key EUV emission that drives atmospheric escape on all types of exoplanets (bottom panels). Combined, the Arcus dataset enables atmospheric evolution (X-ray+EUV) and photochemistry (FUV) models for terrestrial and gaseous planets.

Furthermore, the X-ray/FUV line ratio for ions that emit in both bands (e.g., Fe XIX, Fe XII, and Fe XXI) provides strong diagnostics of coronal temperatures that are independent of the specific ionization state of the plasma. Combining sensitive temperature determination and coronal abundance patterns, Arcus observations will provide empirical data to distinguish between coronal heating models.[42,43]

The Arcus CSS will also include a set of M dwarfs, important for establishing any differences in magnetic activity between main sequence stars with solar-type dynamos and fully convective stars with turbulent dynamos. Surprisingly, no difference has been observed to date in their well-established rotation–activity relation,[44,45] and the planet-hosting red dwarf Proxima Cen even shows a coronal activity cycle.[46] The CSS includes ~5× more fully convective stars than the handful that have been observed to date with X-ray gratings, providing an unprecedented dataset for studies of magnetically heated stellar atmospheres.

Arcus will permit EMD analysis for the full sample of CSS targets. This sample consists of about half of the HWO tier A and B targets (mostly F, G, and K stars), plus the brightest ROentgen SATellite (ROSAT)-detected M dwarfs to increase the sample near the transition to fully convective stars. We note that unless the HWO telescope size is significantly increased, the current HWO target list will change very little because they are the most promising systems drawn from a volume-complete sample. Arcus CSS observations are driven by the exposure time required for high-S/N X-ray observations; UVS spectra will achieve S/N > 15 per resolution element in the peak of the O VI 1032-Å emission line. As most cool stars have transition region temperature distributions peaked at cooler temperatures, this S/N metric ensures that all of the other major FUV emission lines (C III, Si III, H I Lyα, N V, C II, Si IV, and C IV) will be detected at high S/N and readily sub-divided into wavelength-dependent lightcurves for temperature-resolved flare studies (e.g., Refs. 38 and 41). The wide distribution of FUV fluxes in the galactic

stars observed by Arcus drives the bright object capability of the UVS, requiring observations of sources with peak fluxes as bright as 1×10^{-11} erg cm^{-2} s^{-1} Å^{-1}.

3 Arcus Ultraviolet Spectrograph

The UVS requirements motivate an instrument with >5× the effective area and >10× the sensitivity at wavelengths near rest frame and low-redshift O VI (1020 to 1100 Å) than any previous instrument. This is accomplished with an architecture consisting of an off-axis Cassegrain telescope feeding a two-channel imaging spectrograph. UVS's optics are coated in an advanced lithium fluoride (LiF) prescription (e.g., Ref. 47 noting that the final assignment of overcoat will be made in phase A). Data are collected on a photon counting detector and processed on the ground. A rendering of the UVS instrument package is shown in Fig. 4, and the key science measurement requirements and projected performance are shown in Table 1 and Fig. 5. We refer the reader to the companion instrument paper by Fleming et al. (this issue) for instrument design and component-level efficiencies.

The telescope is sized to provide the appropriate collecting area for the Arcus science objectives, with margins of greater than 30% on all major performance parameters to maintain a low-risk posture. The UVS design simultaneously offers spectral resolving power >20,000 and arcsecond-level imaging spectroscopy between 970 and 1580 Å for the first time. The 0.6-m aperture off-axis Cassegrain telescope focuses light into the spectrograph through 6-arcmin–long by 10-arcsec–wide slits. The slit is polished, so the field of view that does not pass to the spectrograph is reflected into the UVS slit camera for added pointing error tracking on the ground. The spectrograph employs two holographically ruled diffraction gratings that can be interchanged to select the G110M (970 to 1250 Å) or G140M (1200 to 1580 Å) wavelength ranges.

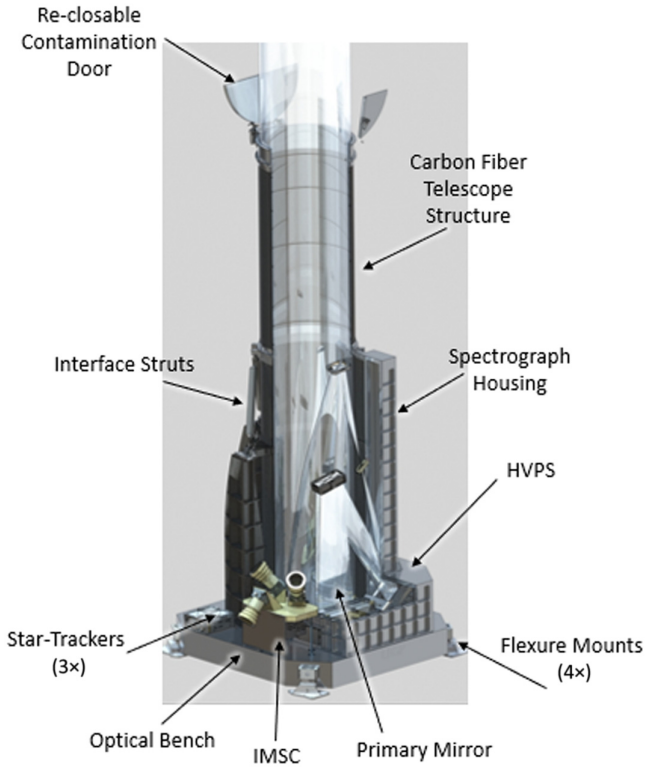

Fig. 4 Schematic of the Arcus UVS instrument package with major components labeled. The three-head star tracker and IMSC controller are mounted on UVS to provide high-fidelity pointing knowledge for image reconstruction. The IMSC comprises the star tracker and associated attitude determination and control system (ADCS) hardware; the high-voltage power supply is the detector high-voltage power supply. We refer the reader to the companion instrument paper by Fleming et al. (this issue) for instrument design and component-level performance predictions.

Table 1 Arcus UVS instrument performance.

Instrument parameter	UVS performance
Spectral bandpass	970 to 1580 Å
Resolving power	24,200
S/N per resolution element at $F_\lambda = 3 \times 10^{-15}$ erg cm^{-2} s^{-1} Å^{-1} in 100 ks	15.6 at 1050 Å, 13.6 averaged over 1032 to 1342 Å
Peak flux limit	3.6×10^{-11} erg cm^{-2} s^{-1} Å^{-1}
FUV absolute flux calibration	5%
Absolute wavelength calibration	34 mÅ

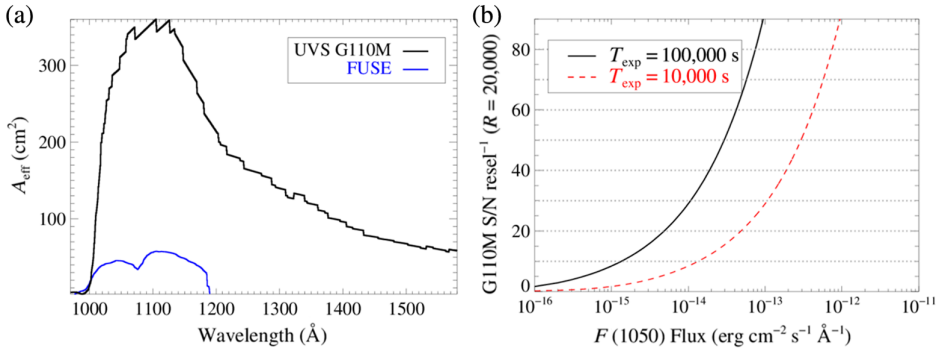

Fig. 5 (a) The Arcus UVS effective area as a function of wavelength is plotted in black. The total FUSE effective area curves [combining LiF and silicon carbide (SiC) channels] at $\lambda > 1000$ Å are shown in blue for comparison. (b) We show the UVS S/N per $R = 20{,}000$ resolution element at 1050 Å ($\Delta\lambda = 0.052$ Å), for typical exposure times of 10 and 100 ks, as a function of point source continuum flux density at 1050 Å.

A toroidal folding mirror provides additional aberration control and long focal length that enables the spectral and spatial resolution performances of the instrument.

The photons are recorded on an open-faced microchannel plate (MCP) detector provided by the University of California, Berkeley, and the photon lists are telemetered to the ground with spacecraft pointing information and offset measurements from a slit-jaw viewing aspect camera. The high resolution of UVS necessitates both stable pointing on short timescales and the ability to correct for pointing and thermal drifts on longer timescales. S/C pointing stability, which impacts the location of the instrument point spread function (PSF) on the detector (and therefore spectral resolution) as a function of time, is better than 0.25-in. RMS for timescales shorter than the spacecraft pointing knowledge timescale. This supports the instrument spectral resolving power performance >20,000 (Table 1). On longer timescales, motions of the PSF at the focal plane are tracked and removed from the data using the photon-counting capability of the MCP detector, as is common for medium-resolution UV spectrographs (e.g., HST-COS instrument handbook[48]). Arcus will mount a three-head star tracker and inertial reference unit [labeled Instrument Mounted Spacecraft Component (IMSC) in Fig. 4] at the end of the UVS telescope baffle tube; the reference pointing error from the trackers is captured at 0.1-s cadence and down-linked with the science data and centroid positions for known stars in the UVS slit camera. The pointing knowledge is used to correct PSF drift as part of the level 2 data pipeline products and maintains spectral resolution across long exposures.

As noted above, the XRS and UVS are co-aligned to simultaneously acquire X-ray and UV spectroscopy of the same astronomical target. The UVS optical axis is established by measuring the angles of optical references relative to the center of the UVS slit during instruments I and T. The UVS and XRS instrument assemblies are referenced to the spacecraft instrument adapter pad

during observatory integration. During on-orbit commissioning, the UVS slit-to-ADCS alignment is established by centering a calibration target in the UVS aperture; the maximum post-deployment offset between the UVS and XRS optical axes are approximately 0.5' and 0.6' in the cross-dispersion and dispersion axes, respectively. If necessary, the XRS alignment and focus mechanism bring the UVS and XRS into the final co-alignment; common calibration sources (e.g., hot white dwarfs) are used to confirm instrument performance in both channels following co-alignment (we refer readers to Cheimets et al. (this issue) for additional details on the Arcus instrument alignment).

4 Arcus UVS General Observing Simulations: Point and Extended Sources

Arcus is first and foremost a General Observer (GO) facility, with >70% of the mission observing time devoted to the pursuit of scientific investigations proposed by the community through regular open time calls. The GO program will capitalize on the discoveries being returned by the ongoing baseline science mission, utilizing these as jumping-off points to design deeper studies. Further, GOs will also leverage the quality of the baseline science data as proof-of-performance inspiration to increase the breadth of Arcus' science yield. In the following sub-sections, we provide data simulations and performance metrics for two hypothetical GO investigations—using star-forming galaxies to augment AGN as probes of galactic halos and spectral mapping observations to build three-dimensional maps of the temperature and kinematics of the warm gas cycling into and out of galaxies.

4.1 Low-Starburst Galaxies: Drivers and Probes of Cosmic Feedback

The 2020 decadal report emphasized the importance of understanding how stellar feedback drives the evolution of cosmic ecosystems (Secs. 1.1.3 and 2.3 of Astro2020[1]). The intense energetic radiation fields, strong stellar winds, and supernova explosions of the most massive stars (O and B stars) dominate the mass, energy, and chemical flows in galaxies. O and B stars ($\approx$5 to 200 $M_\odot$), born in short-lived bursts of star formation, are the strongest drivers of a galaxy's ongoing kinematic and chemical evolution.[49–51] The FUV bandpass contains the most sensitive diagnostics for the spectral type and stellar wind properties of the most massive stars.[52,53] At the same time, these hot star populations can serve as backlights to study the gas in- and outflowing from these galaxies and lower-redshift galactic halos along the line of sight, providing a powerful complement to galactic halo studies using AGN to probe circumgalactic halos.

Arcus UVS will be able to conduct high-S/N spectral observations of low-z star-forming galaxies, measuring mass outflows, stellar populations, interstellar medium of these galaxies, and line-of-sight halo gas. Figure 6 presents a simulation of the FUV spectrum of a $z \approx 0.1$ star-forming galaxy. The target flux is estimated from the low-z FUSE starburst survey of Grimes et al.,[49] with the predicted S/N ($\approx$10 per $R = 24,000$ resolution element) assuming a

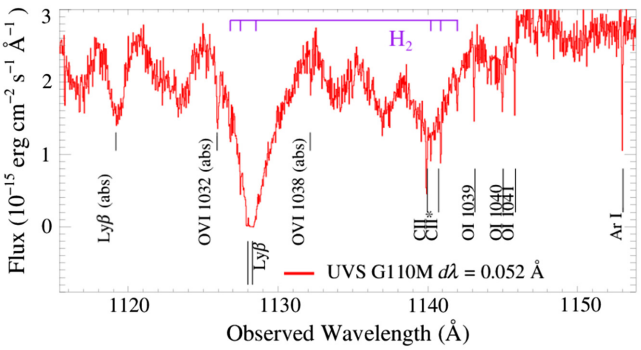

Fig. 6 Simulated spectrum of a $z = 0.1$ star-forming galaxy observed by Arcus UVS. Narrow atomic and molecular lines from the target galaxy ISM are labeled, and an intervening Lyβ and O VI absorption system ($\Delta v \approx -2400$ km s^{-1}) are labeled with the "abs" tag. The simulation is at the expected S/N and spectral resolution (corresponding to $R = 24,000$) for a characteristic 100-ks exposure time.

characteristic 100-ks exposure time in the G110M grating. This simulation shows a somewhat evolved star cluster where the O-type stars have largely died out (removing the strong O VI wind lines from the simulated spectral region) and includes interstellar absorption from neutral and low-ionization metals and H_2. A warm/hot gas absorption system [$T_{abs} = 10^6$ K, $N(\mathrm{O\,VI}) = 6 \times 10^{13}$ cm^{-2}, $N(\mathrm{H\,I}) = 3 \times 10^{14}$ cm^{-2}] is imposed at $\Delta v \approx -2400$ km s^{-1} from the galaxy redshift to demonstrate the line contrast for the detection of intervening halo gas. The column densities were selected to be at the lower edge of the distributions observed in the COS halos[24,54,55] and other surveys (see, e.g., Tumlinson et al.[13] for a review) with a galaxy-absorber velocity offset chosen arbitrarily to be visible on the same high-resolution spectral plot as prominent galactic interstellar features. These same observations would allow for off-planar gas to be observed in the rest of the UVS long slit, which will be discussed in Sec. 4.2.

4.2 Ultraviolet Emission Line Mapping of Galaxies

The use of integral field unit spectroscopy is growing explosively in astrophysics, driven by powerful ground-based instruments (e.g., MUSE[56] and KCWI[57]) as well as JWST. Arcus will uniquely contribute to this approach by providing long-slit UV spectroscopy with excellent angular and spectral resolutions (the filled-slit spectral resolution of the instrument is $R \sim 2000$) in the spectral region at $\lambda < 1150$ Å where high-sensitivity, high-angular resolution spectroscopy has never been conducted. HST surveys such as COS Legacy Spectroscopic SurveY (CLASSY) (e.g., Refs. 58 and 59) have shown that the UV provides a rich variety of emission line diagnostics tracing abundances, physical conditions, and kinematics, but most existing work uses single apertures and does not have spatially resolved emission maps. Figure 7 shows an example of a target that could be mapped with the Arcus+UVS UV long slit. This galaxy (NGC 4631) is known to exhibit widespread O VI emission as shown (see also Refs. 47 and 60), and by sweeping a long slit across the galaxy, the O VI emission can be mapped in detail, thereby revealing the gas physics and kinematics versus location and height above the disk. This unique information directly connects to the galaxy ecosystems/baryon cycle science priority identified by the Astro2020 decadal. The interstellar medium (ISM) and halo of the Milky Way also show extensive emission from O VI and low-ionization stages such as C II* (e.g., Ref. 54), and as every

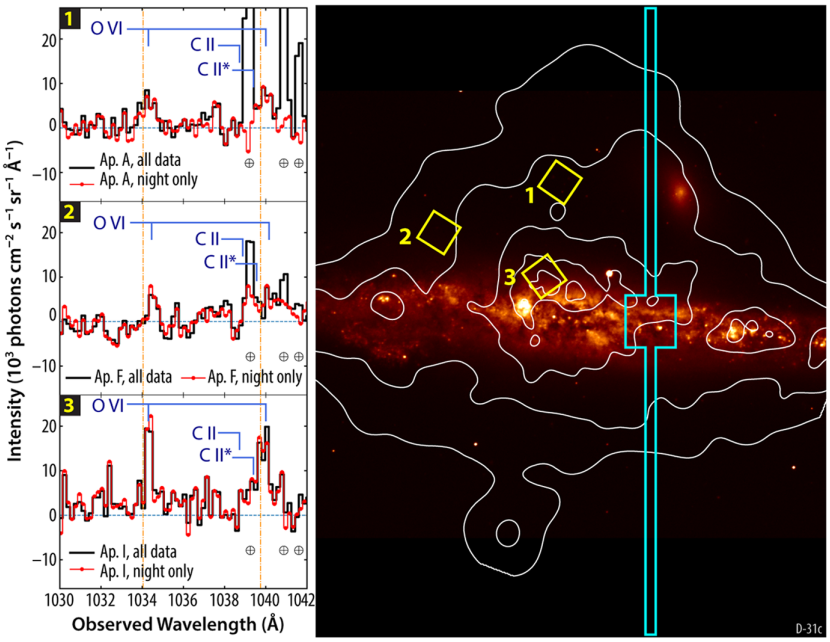

Fig. 7 Sloan Digital Sky Survey g-band image of NGC 4631 with three FUSE apertures (overlaid yellow boxes) that all show O VI emission (see side panels) as well as soft X-ray emission (contours). The UVS long slit (cyan) obtains $R \sim 2500$ to 4000 spectra at arcsecond-level angular resolution along its length.

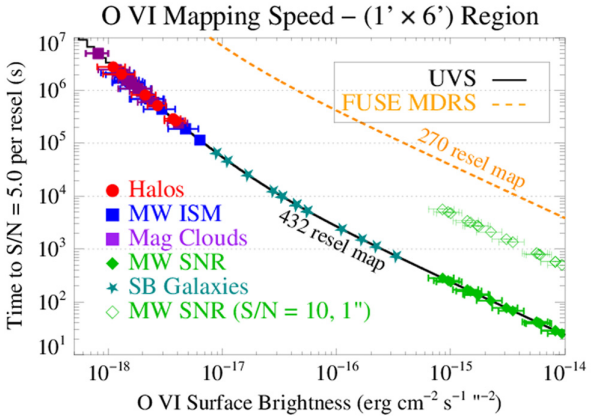

Fig. 8 The mapping speed to S/N = 5 per 10 arcsec × 5 arcsec angular resolution element over a 1 arcmin × 6 arcmin field of view (black) as a function of O VI emission line surface brightness. Arcus is capable of mapping extended FUV emission source factors of 50 to 100 times faster than FUSE (with the 4 arcsec × 20 arcsec MDRS aperture, orange dashed curve). O VI surface brightness from a range of astrophysical environments is shown overplotted on the black curve, from galactic halos (red, blue, and purple points[61–64]) to starburst galaxies (dark teal points[49]) and galactic supernova remnants (green filled diamonds[65,66]). As the mapping times become very short for bright objects, we also show the mapping time with higher signal-to-noise and angular resolution (S/N = 10 per 10 arcsec × 1 arcsec angular resolution) as the open green diamonds in this figure.

Arcus observation will observe the Milky Way gas, likely more than 1000 directions would be observed, providing an extraordinary map of O VI in a variety of locations ranging from the Local Bubble out to the distant galactic halo.

As demonstrated by Otte et al.[61] and Chung et al.,[62] typical O VI surface brightnesses around low-z galaxies, as well as the halo of the Magellanic Clouds and the Milky Way,[63] is B(O VI) ~few × 10^{-18} erg cm^{-2} s^{-1} arcsec^{-2}. Figure 8 illustrates the spectral mapping capability of UVS and compares it to the time required for lower angular resolution spectral mapping with FUSE. Figure 8 plots the exposure time required to map a 1 ft. × 6 ft. region to a depth of S/N = 5 per 10-in. × 5-in.. angular bin. This shows that one could map the entire halo of a galaxy with a surface brightness of ~1.5 × 10^{-18} erg cm^{-2} s^{-1} arcsec^{-2} in approximately 1 Ms, and the bright end of the halo distribution could be mapped in the characteristic 100-ks Arcus exposure time. Also shown are examples of O VI emission from starburst galaxies[49] and galactic supernova remnants,[65,66] which can be accomplished in short observing campaigns. We compare this to the equivalent time to map this angular area with comparable resolution with the FUSE medium resolution (MDRS) aperture (4 arcsec × 20 arcsec). Combining the gain in an effective area with the need to raster 15 × 18 pointings with FUSE compared to 1 × 6 pointings with UVS, Arcus is capable of mapping extended FUV emission sources factors of 50 to 100 times faster than FUSE (and at higher angular resolution for brighter objects) at a filled aperture resolving power of $R > 2000$ to resolve the velocity structure of the outflows. The high-sensitivity and long-slit imaging capability of UVS make possible highly sought-after datasets such as complete maps of O VI (Lyα, C IV, etc.) in a way that was infeasible for previous observatories.

5 Summary

This paper has described the science motivation and performance of the Arcus UVS, a 60-cm, off-axis Cassegrain telescope feeding an imaging spectrograph operating over the 970- to 1580-Å bandpass. The instrument employs two interchangeable diffraction gratings to provide medium-resolution spectroscopy ($R > 20{,}000$ in two grating modes centered at ~1110 and 1390 Å, respectively). We presented example science cases and data simulations showing how the capabilities of UVS address a broad range of science questions highlighted by the 2020 Astronomy and Astrophysics Decadal Survey, from the temperature and composition of the missing baryons in the intergalactic medium to the evolution of stars and their influence on orbiting planets. Arcus was submitted to NASA's inaugural Astrophysics Probe solicitation in late 2023.

Code and Data Availability

The data utilized in this study were obtained from the Mikulski Archive for Space Telescopes and the authors; they can be requested from the author at kevin.france@colorado.edu.

Acknowledgments

A portion of the results presented in this work previously appeared in SPIE proceeding 2023SPIE12678E.0FF.

References

1. National Academies of Sciences, E. and Medicine, *Pathways to Discovery in Astronomy and Astrophysics for the 2020s*, The National Academies Press, Washington, DC (2021).
2. T. Di Matteo, V. Springel, and L. Hernquist, "Energy input from quasars regulates the growth and activity of black holes and their host galaxies," *Nature* **433**, 604–607 (2005).
3. J. Magorrian et al., "The demography of massive dark objects in galaxy centers," *Astron. J.* **115**, 2285–2305 (1998).
4. L. Ferrarese and D. Merritt, "A fundamental relation between supermassive black holes and their host galaxies," *Astrophys. J.* **539**, L9–L12 (2000).
5. J. S. Kaastra et al., "X-ray absorption lines in the Seyfert 1 galaxy NGC 5548 discovered with Chandra-LETGS," *Astron. Astrophys.* **354**, L83–L86 (2000).
6. S. Kaspi et al., "The ionized gas and nuclear environment in NGC 3783. I. Time-averaged 900 kilosecond Chandra grating spectroscopy," *Astrophys. J.* **574**, 643–662 (2002).
7. T. J. Turner et al., "Tracing a disk wind in NGC 3516," *Astron. Astrophys.* **483**, 161–169 (2008).
8. L. C. Gallo, J. M. Miller, and E. Costantini, "Active galactic nuclei with high-resolution X-ray spectroscopy," arXiv:2302.10930 (2023).
9. A. Danehkar et al., "The ultra-fast outflow of the Quasar PG 1211+143 as viewed by time-averaged Chandra grating spectroscopy," *Astrophys. J.* **853**, 165 (2018).
10. G. A. Kriss et al., "Discovery of an ultraviolet counterpart to an ultrafast X-ray outflow in the Quasar PG 1211 + 143," *Astrophys. J.* **853**, 166 (2018).
11. R. J. Weymann et al., "Comparisons of the emission-line and continuum properties of broad absorption line and normal Quasi-Stellar objects," *Astrophys. J.* **373**, 23 (1991).
12. A. L. King et al., "Regulation of black hole winds and jets across the mass scale," *Astrophys. J.* **762**, 103 (2013).
13. J. Tumlinson, M. S. Peeples, and J. K. Werk, "The circumgalactic medium," *Annu. Rev. Astron. Astrophys.* **55**, 389–432 (2017).
14. C. Péroux and J. C. Howk, "The cosmic baryon and metal cycles," *Annu. Rev. Astron. Astrophys.* **58**, 363–406 (2020).
15. J. J. Davies et al., "The quenching and morphological evolution of central galaxies is facilitated by the feedback-driven expulsion of circumgalactic gas," *Mon. Not. R. Astron. Soc.* **491**, 4462–4480 (2020).
16. C. Lochhaas et al., "Fast winds drive slow shells: a model for the circumgalactic medium as galactic wind-driven bubbles," *Mon. Not. R. Astron. Soc.* **481**, 1873–1896 (2018).
17. G. M. Voit, "Ambient column densities of highly ionized oxygen in precipitation-limited circumgalactic media," *Astrophys. J.* **880**, 139 (2019).
18. Y. Faerman et al., "Exploring the Milky Way circumgalactic medium in a cosmological context with a semianalytic model," *Astrophys. J.* **928**, 37 (2022).
19. Y. Faerman and J. K. Werk, "The cool circumgalactic medium of low-redshift star-forming galaxies. I. Empirical model and mean properties," *Astrophys. J.* **956**, 92 (2023).
20. J. X. Prochaska et al., "The COS-Halos survey: metallicities in the low-redshift circumgalactic medium," *Astrophys. J.* **837**, 169 (2017).
21. B. D. Oppenheimer and J. Schaye, "Non-equilibrium ionization and cooling of metal-enriched gas in the presence of a photoionization background," *Mon. Not. R. Astron. Soc.* **434**, 1043–1062 (2013).
22. E. Hodges-Kluck, J. Cafmeyer, and J. N. Bregman, "Ultraviolet halos around spiral galaxies. I. Morphology," *Astrophys. J.* **833**, 58 (2016).
23. M. S. Peeples et al., "A budget and accounting of metals at $z \sim 0$: results from the COS-Halos survey," *Astrophys. J.* **786**, 54 (2014).
24. J. K. Werk et al., "The COS-Halos survey: origins of the highly ionized circumgalactic medium of star-forming galaxies," *Astrophys. J.* **833**, 54 (2016).
25. S. Walsh, "Detection capabilities of the Athena X-IFU for the warm-hot intergalactic medium using gamma-ray burst X-ray afterglows," *Astron. Astrophys.* **642**, A24 (2020).
26. C. Garraffo et al., "The threatening magnetic and plasma environment of the TRAPPIST-1 planets," *Astrophys. J. Lett.* **843**, L33 (2017).

27. K. France et al., "The high-energy radiation environment around a 10 Gyr M dwarf: habitable at last?," *Astron. J.* **160**, 237 (2020).
28. J. E. Owen, "Atmospheric escape and the evolution of close-in exoplanets," *Annu. Rev. Earth Planet. Sci.* **47**, 67–90 (2019).
29. K. J. Zahnle and D. C. Catling, "The cosmic shoreline: the evidence that escape determines which planets have atmospheres, and what this may mean for Proxima Centauri B," *Astrophys. J.* **843**, 122 (2017).
30. C. E. Harman et al., "Abiotic O_2 levels on planets around F, G, K, and M stars: possible false positives for life?," *Astrophys. J.* **812**, 137 (2015).
31. G. N. Arney et al., "Pale orange dots: the impact of organic haze on the habitability and detectability of Earthlike exoplanets," *Astrophys. J.* **836**, 49 (2017).
32. J. Christiansen et al., "Understanding exoplanet atmospheres with UV observations I: NUV and blue/optical," *Bull. Am. Astron. Soc.* **51**, 408 (2019).
33. K. France et al., "The MUSCLES treasury survey. I. Motivation and overview," *Astrophys. J.* **820**, 89 (2016).
34. T. Richey-Yowell et al., "HAZMAT. VIII. A spectroscopic analysis of the ultraviolet evolution of K stars: additional evidence for K dwarf rotational stalling in the first gigayear," *Astrophys. J.* **929**, 169 (2022).
35. P. R. Behr et al., "The MUSCLES extension for atmospheric transmission spectroscopy: UV and X-ray host-star observations for JWST ERS & GTO targets," *Astron. J.* **166**, 35 (2023).
36. K. Poppenhaeger and S. J. Wolk, "Indications for an influence of hot Jupiters on the rotation and activity of their host stars," *Astron. Astrophys.* **565**, L1 (2014).
37. K. France et al., "Far-ultraviolet activity levels of F, G, K, and M dwarf exoplanet host stars," *Astrophys. J.* **239**, 16 (2018).
38. A. Youngblood et al., "EUV influences on exoplanet atmospheric stability and evolution," *Bull. Am. Astron. Soc.* **51**, 320 (2019).
39. V. Kashyap and J. J. Drake, "Markov-chain Monte Carlo reconstruction of emission measure distributions: application to solar extreme-ultraviolet spectra," *Astrophys. J.* **503**, 450–466 (1998).
40. G. M. Duvvuri et al., "Reconstructing the extreme ultraviolet emission of cool dwarfs using differential emission measure polynomials," *Astrophys. J.* **913**, 40 (2021).
41. K. P. Dere et al., "CHIANTI—an atomic database for emission lines. IX. Ionization rates, recombination rates, ionization equilibria for the elements hydrogen through zinc and updated atomic data," *Astron. Astrophys.* **498**, 915–929 (2009).
42. P. J. Cargill and J. A. Klimchuk, "Nanoflare heating of the corona revisited," *Astrophys. J.* **605**, 911–920 (2004).
43. J. M. Laming, "The first ionization potential effect from the ponderomotive force: on the polarization and coronal origin of Alfvén waves," *Astrophys. J.* **844**, 153 (2017).
44. N. J. Wright and J. J. Drake, "Solar-type dynamo behaviour in fully convective stars without a tachocline," *Nature* **535**, 526–528 (2016).
45. M. K. Browning, "Simulations of dynamo action in fully convective stars," *Astron. Astrophys.* **676**, 1262–1280 (2008).
46. B. J. Wargelin et al., "Optical, UV, and X-ray evidence for a 7-yr stellar cycle in Proxima Centauri," *Mon. Not. R. Astron. Soc.* **464**, 3281–3296 (2017).
47. L. Rodríguez-de Marcos et al., "Advanced Al/eLiF mirrors for the SPRITE CubeSat," *Proc. SPIE* **12188**, 1218820 (2022).
48. Cosmic Origins Spectrograph Instrument Handbook for Cycle 32, Version 16 – December 2023, https://hst-docs.stsci.edu/cosihb.
49. J. P. Grimes et al., "Observations of starburst galaxies with far-ultraviolet spectrographic explorer: galactic feedback in the local universe," *Astrophys. J.* **181**, 272–320 (2009).
50. C. Kobayashi and N. Nakasato, "Chemodynamical simulations of the Milky Way galaxy," *Astrophys. J.* **729**, 16 (2011).
51. N. Langer, "Presupernova evolution of massive single and binary stars," *Annu. Rev. Astron. Astrophys.* **50**, 107–164 (2012).
52. A. Pellerin et al., "An atlas of galactic OB spectra observed with the far ultraviolet spectroscopic explorer," *Astrophys. J. Suppl. Ser.* **143**, 159–200 (2002).
53. M. A. Smith, "A detailed far-ultraviolet spectral atlas of O-type stars," *Astrophys. J.* **202**, 17 (2012).
54. J. Tumlinson et al., "The large, oxygen-rich halos of star-forming galaxies are a major reservoir of galactic metals," *Science* **334**, 948 (2011).
55. J. Tumlinson et al., "The COS-Halos survey: rationale, design, and a census of circumgalactic neutral hydrogen," *Astrophys. J.* **777**, 59 (2013).
56. R. Bacon et al., "The MUSE second-generation VLT instrument," *Proc. SPIE* **7735**, 773508 (2010).

57. P. Morrissey et al., "The Keck Cosmic Web Imager integral field spectrograph," *Astrophys. J.* **864**, 93 (2018).
58. D. A. Berg et al., "The COS Legacy Archive Spectroscopy Survey (CLASSY) treasury atlas," *Astrophys. J.* **261**, 31 (2022).
59. X. Xu et al., "CLASSY. VI. The density, structure, and size of absorption-line outflows in starburst galaxies," *Astrophys. J.* **948**, 28 (2023).
60. M. A. MacGregor et al., "Discovery of an extremely short duration flare from Proxima Centauri using millimeter through far-ultraviolet observations," *Astrophys. J. Lett.* **911**, L25 (2021).
61. B. Otte et al., "Probing O VI emission in the halos of edge-on spiral galaxies," *Astrophys. J.* **591**, 821–826 (2003).
62. H. Chung, C. J. Vargas, and E. Hamden, "Revisiting FUSE O VI emission in galaxy halos," *Astrophys. J.* **916**, 7 (2021).
63. W. V. Dixon and R. Sankrit, "The FUSE survey of diffuse O VI emission from the interstellar medium," *Am. Inst. Phys. Conf. Ser.* **1156**, 130–134 (2009).
64. W. V. D. Dixon, R. Sankrit, and B. Otte, "An extended FUSE survey of diffuse O VI emission in the interstellar medium," *Astrophys. J.* **647**, 328–349 (2006).
65. R. Sankrit, W. P. Blair, and J. C. Raymond, "Optical and far-ultraviolet spectroscopy of knot D in the Vela supernova remnant," *Astrophys. J.* **589**, 242–252 (2003).
66. R. Sankrit et al., "Far ultraviolet spectroscopic explorer spectroscopy of the XA region in the Cygnus Loop supernova remnant," *Astron. J.* **133**, 1383–1392 (2007).

Kevin France is a professor at LASP/University of Colorado. Kevin France's research focuses on exoplanets, their host stars, and the development of instrumentation for ultraviolet astrophysics. He is the principal investigator (PI) of the Extreme-ultraviolet Stellar Characterization for Atmospheric Physics and Evolution (ESCAPE) Small Explorer concept, NASA's Colorado Ultraviolet Transit Experiment (CUTE) mission, and a NASA-supported sounding rocket to flight-test critical path hardware for future UV/optical astrophysics missions. He was a member of the HST-COS and Habitable Worlds Observatory (HWO) Science, Technology, & Architecture Review Team (START) teams, and the study PI for the Large Ultraviolet/Optical/Infrared Surveyor (LUVOIR) ultraviolet spectrograph.

Laura Brenneman is the division chair for high-energy astrophysics at the Center for Astrophysics (CfA) and the deputy PI for Arcus. Her research focuses on observing the innermost regions around supermassive black holes, studying inflows via accretion and outflows via winds. She is also a co-investigator on the X-Ray Imaging and Spectroscopy Mission (XRISM) mission and the lone US representative on European Space Agency's (ESA's) NewAthena Science Study Team, as well as a member of the calibration teams for both missions.

Nancy Brickhouse is a senior astrophysicist in the Solar, Stellar, and Planetary Division at the CfA and the lead scientist for stars for Arcus. Her research focuses on high-energy emissions from collisionally ionized plasmas, including stellar coronae and young star accretion streams. She conducts critical evaluations of atomic data used in astrophysics and is a member of the AtomDB team, which curates the publicly available atomic database AtomDB.

Hans Moritz Günther is a research scientist at the Massachusetts Institute of Technology (MIT). He received his undergraduate degree (in 2005) and his PhD (in 2009) in physics from the University of Hamburg, Germany. After that, he worked at the Harvard-Smithsonian Center for Astrophysics and came to MIT in 2015. He is currently the lead developer of Model of AXAF Response to X-Rays (MARX), the ray-tracing software used for the Chandra X-ray observatory. His science interests are in star formation using data from the radio to X-rays.

Dolon Bhattacharyya is a research scientist at LASP/University of Colorado. Her research focuses on studying atmospheric escape from the upper atmospheres of planets. She is the PI of several HST proposals, has served as the project scientist for the Carruthers Geocorona Mission (CGO), and has been a part of the Mars Atmosphere and Volatile EvolutioN - Imaging Ultraviolet Spectrograph (MAVEN-IUVS) science team. She has also led/been involved with UV detector calibration efforts for HST's Advanced Camera for Surveys-Solar Blind Channel (ACS-SBC) instrument, CGO, and the MAVEN-IUVS echelle channel.

Pasquale Temi is a scientist at NASA – Ames Research Center. He has extensive experience in multi-wavelength data acquisition, analysis, and interpretation of observations of active galactic nucleus feeding and feedback processes in groups and galaxy clusters. He successfully planned, managed, and executed observations with Chandra, Spitzer, Herschel, Atacama Large Millimeter Array (ALMA), Stratospheric Observatory for Infrared Astronomy (SOFIA), and JWST.

Biographies of the other authors are not available.